Rib cage mechanics during quiet breathing and exercise in humans

C. M. KENYON,[1] S. J. CALA,[1] S. YAN,[2] A. ALIVERTI,[3]
G. SCANO,[4] R. DURANTI,[4] A. PEDOTTI,[3] AND PETER T. MACKLEM[1]
[1]*Meakins-Christie Laboratories, McGill University, and* [2]*Montréal Chest Institute, Montreal, Quebec, Canada H2X 2P4;* [3]*Politecnico di Milano, Dipartimento di Bioingegneria, Centro di Bioingegneria, Milan; and* [4]*First Clinica Medica III, Università di Firenze, Florence, Italy*

Kenyon, C. M., S. J. Cala, S. Yan, A. Aliverti, G. Scano, R. Duranti, A. Pedotti, and Peter T. Macklem. Rib cage mechanics during quiet breathing and exercise in humans. *J. Appl. Physiol.* 83(4): 1242–1255, 1997.—During exercise, large pleural, abdominal, and transdiaphragmatic pressure swings might produce substantial rib cage (RC) distortions. We used a three-compartment chest wall model (*J. Appl. Physiol.* 72: 1338–1347, 1992) to measure distortions of lung- and diaphragm-apposed RC compartments (RCp and RCa) along with pleural and abdominal pressures in five normal men. RCp and RCa volumes were calculated from three-dimensional locations of 86 markers on the chest wall, and the undistorted (relaxation) RC configuration was measured. Compliances of RCp and RCa measured during phrenic stimulation against a closed airway were 20 and 0%, respectively, of their values during relaxation. There was marked RC distortion. Thus nonuniform distribution of pressures distorts the RC and markedly stiffens it. However, during steady-state ergometer exercise at 0, 30, 50, and 70% of maximum workload, RC distortions were small because of a coordinated action of respiratory muscles, so that net pressures acting on RCp and RCa were nearly the same throughout the respiratory cycle. This maximizes RC compliance and minimizes the work of RC displacement. During quiet breathing, plots of RCa volume vs. abdominal pressure were to the right of the relaxation curve, indicating an expiratory action on RCa. We attribute this to passive stretching of abdominal muscles, which more than counterbalances the insertional component of transdiaphragmatic pressure.

respiratory kinematics; respiratory muscles; rib cage distortions; rib cage bending stiffness; diaphragm

DURING EXERCISE, large respiratory pressure swings are generated that result in highly nonuniform pressures in the pleural space over the inner surface of the rib cage. The pressure over the lung-apposed or pulmonary part of the rib cage is pleural pressure (Ppl) over the costal surface of the lung, which falls during inspiration, whereas over the diaphragm-apposed or abdominal part, Ppl is approximated by abdominal pressure (Pab) (20), which normally rises during a quiet inspiration. In addition, the diaphragm and some of the abdominal muscles insert directly onto ribs 7–12 and have inflationary and deflationary actions, respectively, on the abdominal but not on the pulmonary part of the rib cage. Nondiaphragmatic inspiratory muscles (scalenes, parasternal intercostals, and sternocleidomastoids) insert on ribs 1–6 and have inflationary actions on the pulmonary but not on the abdominal part (3, 9, 31). Rib cage distortions caused by these nonuniform pressures and the resultant restoring forces are unknown in exercise but have been measured during isolated diaphragmatic contractions and quiet breathing (9, 31). We use an extension of the two-compartment model of the rib cage used previously (31) to calculate rib cage distortions and restoring forces during exercise.

Unitary behavior of the rib cage requires that the net pressures acting on the two rib cage compartments be equal, and this would require considerable coordination of the respiratory muscles. Thus it is not surprising that several studies have shown various degrees of departure from the undistorted configuration of the rib cage during increased respiratory efforts (27, 28) and in quiet breathing (21, 31). All these studies have assessed distortion by measuring rib cage dimensions or cross-sectional areas. Although from a respiratory point of view, compartmental volume change or lack of it is the most crucial variable, it has not been possible to measure the volume of chest wall compartments directly. Recently, an optical tracking device (ELITE) has been developed that can give the three-dimensional location of many markers with the high temporal (100 Hz) and spatial accuracy ($\pm$0.2 mm) required for respiratory measurements (5, 13). We have used this device with a configuration of marker points (5) designed specifically to measure the volume of three chest wall compartments, the pulmonary and abdominal rib cage compartments and the abdomen, directly.

We report rib cage distortions measured by displacements of the pulmonary and abdominal rib cage compartments away from their undistorted relaxation configurations during exercise at various power outputs. From the measured distortions, we calculate the restoring forces (expressed as a pressure) and, knowing these, the pressures developed by the nondiaphragmatic inspiratory muscles. These pressures have not been measured, except during quiet breathing (31).

To make these measurements, we model the two rib cage compartments mechanically coupled to each other, with nondiaphragmatic inspiratory muscles acting on the pulmonary rib cage and the diaphragm and abdominal muscles acting on the abdominal rib cage. This model extends that of Ward et al. (31) by including the actions of abdominal muscles on the abdominal rib cage. These were not previously estimated, inasmuch as only quiet breathing was being studied when expiratory muscles were minimally activated. We use a normalization for rib cage distortion (9) so different subjects can be directly compared for distortability and for the amount of distortion during exercise.

Glossary

ABM,ins	Abdominal muscles acting to deflate RCa
ABM,nins	Abdominal muscles with no action on RCa
C	Static compliance of rib cage compartments measured during relaxation
C′	Dynamic compliance of rib cage compartments measured during bilateral phrenic nerve stimulation
FRC	Functional residual capacity
Pab	Abdominal pressure
Pabm	Pressure developed by abdominal muscles (Pab − Pabw)
Pabw	Elastic recoil pressure of abdomen
Pbs	Body surface pressure
Pdi	Transdiaphragmatic pressure (Pab − P_x + P_x − Ppl, as measured by Pga − Pes)
Pes	Esophageal pressure
Pga	Gastric pressure
P_{link}	Restoring pressure acting to diminish rib cage distortion, which arises from distortions away from relaxation configuration of RCp and RCa and bending stiffness of the rib cage
Pm	Mouth pressure
Ppl	Pleural pressure
Prc,a	Elastic recoil pressure of RCa
Prcm	Pressure developed by rib cage muscles
Prc,p	Elastic recoil pressure of RCp
P_v	Net pressure acting on RCp resulting from Ppl + Prcm before effects of distortion are taken into account
P_w	Net pressure acting on RCa before effects of distortion resulting from (P_x − Ppl) + (Pab − P_y) are taken into account
P_x	Imaginary pressure between Pab and Ppl; it partitions Pdi into a costal component (P_x − Ppl) and a crural component (Pab − P_x)
P_y	Imaginary pressure between Pab and Pabw; it partitions Pabm into an insertional component (P_y − Pabw), which has a deflationary action on RCa, and a noninsertional component (Pab − P_y), which has no action on RCa
RCa	Abdominal or diaphragm-apposed rib cage
RCp	Pulmonary or lung-apposed rib cage
T_I	Inspiratory time
Vab	Volume of abdomen
V_L	Lung volume
Vrc,a	Volume of RCa
$\dot{V}$rc,p	Volume of RCp
$\dot{W}$max	Maximum exercise workload
*x*Pdi	Insertional component of Pdi or fraction of Pdi that has a direct inflating action on RCa, where $0 \leq x \leq 1$
*y*Pabm	Insertional component of Pabm, where $0 \leq y \leq 1$

METHODS

Model. The rib cage model of Ward et al. (31) divides the rib cage into pulmonary (RCp) and abdominal (RCa) compartments. We define RCp as the part of the rib cage apposed to the lung and RCa as the part apposed to the diaphragm. To measure their volumes (Vrc,p and Vrc,a) from surface markers, we defined the boundaries of RCp as extending from the clavicles to a line extending transversely around the thorax at the level of the xiphisternum and RCa as extending from this line to the lower costal margin. We define the undistorted rib cage configuration as the relationship between Vrc,p and Vrc,a when all respiratory muscles are relaxed and (neglecting gravitational effects) Ppl and Pab are equal, so that the pressure difference across the rib cage is uniform.

Figure 1 shows a hydraulic or electrical model that extends the model of Ward et al. (31). It is a lumped-parameter model in which, common to most other models of the mechanics of breathing (2, 6, 19, 26), the respiratory muscles act to displace the various compartments of the respiratory system (lungs, rib cage, and abdomen). Pressures are quantified as the difference between active and relaxation pressures at any lung volume (V_L) (6, 26). In our model, rectangles are used for loads on the system (impedances), ovals and circles indicate pressure generators, and hexagons and diamonds indicate summing junctions outputting the algebraic sum of their signed inputs. Above each pressure generator is an arrow to indicate in what direction it increases pressure. We use a sign convention whereby the pressure generated by a muscle is positive. The summing junction in the shaded area determines the pressures producing rib cage distortion as the difference in the net pressures acting on RCp and RCa. This produces a restoring force depending on the degree of distortion and the bending stiffness of the rib cage (8, 31), which we refer to as P_{link}. This acts when the rib cage is distorted away from its relaxed configuration. The output of this summing junction indicated by the open arrowhead is P_{link}, which operates in opposite directions on the upper and lower rib cages. It is presumably generated as a torque acting on ribs that span the abdominal and pulmonary rib cage compartments. (This was implicit in the original description of Ward et al. but was not stated explicitly.) We have also added the abdominal muscles divided functionally and anatomically into two groups: ABM,ins are the abdominal muscles that act directly to deflate the lower rib cage (e.g., external oblique), and ABM,nins are the abdominal muscles that do not act directly on the lower rib cage (e.g., transversus). This is directly analogous to dividing transdiaphragmatic pressure (Pdi) into an insertional component, which acts directly on the rib cage (P_x − Ppl in the model), and a noninsertional component, which does not (Pab − P_x). ABM,ins acts hydraulically in series with ABM,nins to displace the abdomen inward and to increase Pab, which is transmitted through the diaphragm to act at the inner surface of RCa in the area of apposition of the diaphragm to the rib cage. This inflationary action of Pab on RCa is counterbalanced by the deflating action of ABM,ins given by P_y − Pabw. Pabw is the elastic recoil pressure of the abdominal wall, and P_y (analogous to P_x) is an imaginary pressure partitioning the total pressure developed by abdominal muscles (Pabm) into an insertional (P_y − Pabw) and a noninsertional (Pab − P_y) component. The role of the abdominal muscles and their actions during exercise are extensively discussed elsewhere (3). However, there is an important distinction between our model of the abdomen and previous models. To the best of our knowledge, all previous models have stated that the elastic recoil pressure of the abdomen is given by Pab relative to body surface

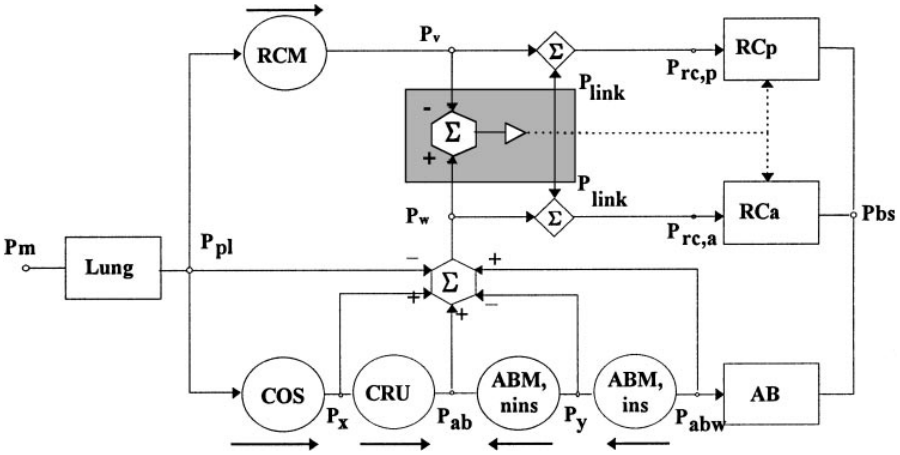

Fig. 1. Electrical model of 2-compartment rib cage [pulmonary (RCp) and abdominal (RCa)] and abdomen (AB). Circles represent pressure generators, which increase pressure in direction indicated by arrow above each generator. Ovals indicate impedances, and hexagons and diamonds represent summing junctions. Inputs to summing junctions are signed to indicate effect on junction of pressure increases from each of inputs. Summing junction in shaded area determines net difference in pressure acting on RCp and RCa, which produces rib cage distortion. Output of this junction (open arrowhead) is restoring force represented by a pressure (P_{link}) that acts in opposite directions on RCp and RCa. Dotted line to RCp and RCa indicates that distortion of rib cage affects compliance of rib cage compartments. P_v, imaginary pressure on RCp before effect of rib cage distortion is taken into account; P_w, analogous pressure for RCa; P_x and P_y, imaginary pressures between parts of muscles with different actions as indicated by model; Pm, mouth pressure; Pbs, pressure at body surface; Pabw, pressure from passive stretching of abdominal wall; RCM, rib cage muscles; P_{link}, restoring pressure; Prc,p, elastic recoil pressure of RCp; Prc,a, elastic recoil pressure of RCa; Ppl, pleural pressure; COS, costal part of diaphragm; CRU, crural part of diaphragm; Pab, abdominal pressure; ABM,nins, abdominal muscles with no action on RCa; ABM,ins, abdominal muscles acting to deflate RCa.

pressure (Pbs) (12, 14, 16). Thus the elastic recoil of the abdomen includes passive stretching of the abdominal muscles. We specifically do not include passive stretching of abdominal muscles as contributing to the elastic recoil of the abdominal wall in our hydraulic model. Thus we take Pabw relative to body surface pressure as the elastic recoil pressure, not Pab, as in previous models.

Following Ward et al. (31), we can now describe the pressures developed by various muscles and write pressure balance equations. Pdi is given by the sum of the pressures acting across the costal and crural parts of the diaphragm (12, 19): $Pdi = (Pab - P_x) + (P_x - Ppl)$. We assume that the insertional component of Pdi ($P_x - Ppl$) is a constant fraction of Pdi and can be represented as xPdi, where $0 \geq x \geq 1$. Similarly, we assume that the insertional component of abdominal muscles ($P_y - Pabw$) is a constant fraction of the total pressure developed by the abdominal muscles ($Pabm = Pab - Pabw$) and can be represented by yPabm, where $0 \geq y \geq 1$. Thus the pressure acting on RCa before the contribution of distortion (P_{link}) is taken into account is the output (P_w) of the lowermost summing junction

$$P_w = -Ppl + P_x + Pab - P_y + Pabw = x\text{Pdi} + Pab - y\text{Pabm} \quad (1)$$

The pressure on the upper rib cage (P_v) before the contribution of distortion is taken into account is simply

$$P_v = Ppl + Prcm \quad (2)$$

where Prcm is the pressure developed by the rib cage muscles on RCp.

Deformation of the rib cage away from its undistorted configuration will result in a restoring pressure (P_{link}) that is of equal magnitude, but opposite sign, on the upper and lower rib cages, but this will not necessarily make the total pressures acting on RCp and RCa equal. This depends on how distorting pressure is transduced into distortion, which then results in a restoring pressure. The total pressures on RCp and RCa are given by

$$P_v - P_{link} = Prc,p$$

$$P_w + P_{link} = Prc,a$$

which at equilibrium are balanced by the elastic recoil of RCp and RCa. Thus Prc,p and Prc,a are the elastic recoil pressures of their respective rib cage compartments.

We define the undistorted configuration of the rib cage as that occurring during relaxation when Pdi, Pabm, and Prcm are zero and, neglecting gravitational effects, Ppl = Pab, so that the pressure difference across the entire rib cage is uniform. As stated by Ward et al. (31), rib cage distortion is the result of a difference in the pressures acting on RCp and RCa; thus subtracting *Eq. 2* from *Eq. 1*

$$(P_w - P_v) = (Pab + x\text{Pdi} - y\text{Pabm}) - (Ppl + Prcm) \quad (3)$$

During phrenic stimulation, Pabm = 0, Prcm = 0, and we obtain

$$(P_w - P_v) = (x + 1)\text{Pdi}$$

Now x is unknown, but as previously described (31), Pdi is proportional to the pressure difference causing distortion. The magnitude of P_{link} depends on how this pressure is transduced into distortion and the bending stiffness of the rib cage.

We measured rib cage distortion on a plot of Vrc,p vs. Vrc,a first during relaxation at different V_L to obtain the undistorted configuration and then by measuring the perpendicular distance of the distorted configuration away from the relaxation line divided by the value of Vrc,p at the intersec-

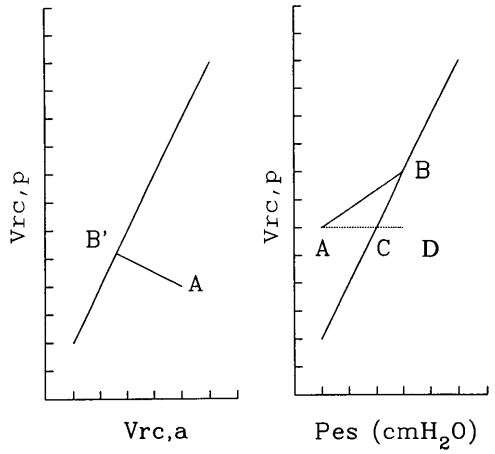

Fig. 2. Definition of rib cage distortion and resulting P_{link} calibrated when only diaphragm is active: long diagonal line represents relaxation characteristic of rib cage. *Left*: relaxation (undistorted) configuration of rib cage is given by long line with positive slope. Rib cage distortion at *point A* relative to relaxation line that goes through *B′* is length *AB′* perpendicular to relaxation line divided by volume of RCp (Vrc,p) at *B′* taken as a percentage, as in Chihara et al. (9). Vrc,a, volume of RCa. *Right*: relaxation pressure-volume curve of RCp is given by long line with positive slope. During phrenic stimulation, RCp follows pathway *BA*; *point B*, Vrc,p at functional residual capacity. *CD*, change in Prc,p during twitch; *DA*, change in esophageal pressure (Pes). Inasmuch as $\Delta Prc,p = \Delta Ppl + P_{link}$, $P_{link} = AC$.

tion point. This results in a dimensionless number that when multiplied by 100 gives percent distortion (Fig. 2, *left*) (9). Distortions were measured during bilateral, transcutaneous, phrenic nerve twitches (electrical stimulation) when the only muscle active was the diaphragm. Rib cage distortability was calculated as a percent distortion divided by ΔPdi, which is proportional to the difference in pressure acting on each compartment (9, 31).

Under equilibrium conditions, Prc,p when RCp is displaced off its relaxation line is balanced by other pressures acting on it. Thus

$$Prc,p = Ppl + Prcm + P_{link} \quad (4)$$

From the relationships between Vrc,p and Ppl during relaxation when Prcm and P_{link} are zero, we obtained Prc,p as a function of Vrc,p. During phrenic stimulation, Prcm = 0, so the pressure balance equation simplifies to

$$Prc,p = Ppl + P_{link}$$

We solved for P_{link} graphically, as shown in Fig. 2, *right*. During breathing we measured the distortion, and from a plot of distortion vs. P_{link} we estimated P_{link} throughout the breath, along with Vrc,p and Ppl. Thus Prcm can be solved for as the only unknown in *Eq. 4*.

Subjects and experimental protocol. We studied five normal men. They were 31–38 yr of age, were free of respiratory disease, and had normal diaphragm function, which we verified before the experiment with bilateral phrenic stimulation and observation of muscle action potentials from surface electrodes. Their anthropometric characteristics are given in Table 1. In each subject on an occasion separate from the main experiment, individual maximum workload ($\dot{W}$max) was assessed by an incremental exercise test on a cycle ergometer by increasing the work rate by 50-W steps until exhaustion, which was at 250–300 W, depending on the subject. Esophageal (Pes) and gastric (Pga) pressures were measured with conventional balloon catheters and were used as indexes of Ppl and Pab. Rib cage distortability was assessed by bilateral transcutaneous phrenic stimulation at increasing intensities to obtain a range of distortions.

Data were gathered during an incremental exercise test on a cycle ergometer while the subject was breathing quietly, pedaling with no load (0% $\dot{W}$max), and exercising at 30, 50, and 70% $\dot{W}$max. Each level was maintained for 3 min and 20 s, and data were acquired during the last 20 s of each level. Subjects breathed on a mouthpiece attached to a three-way valve, one way going to a water displacement spirometer with a CO_2 absorber and the other to room air. The subject was switched from room air to the spirometer for the last 20 s at each level, and the bell was refreshed with room air during the other 3 min. This was used to provide a check on the changes in V_L calculated from the body surface markers. Compartmental volume displacements were assessed from surface markers that were optically tracked in three dimensions, and rib cage volumes were subsequently calculated (5). While the subjects were seated on the cycle ergometer, their forearms were supported away from the sides of the body comfortably below shoulder height, allowing markers on the body surface to be tracked in three dimensions by television cameras in front of and behind them.

Compartmental volume measurements. Volumes were measured directly from the movements of surface markers on the chest wall using an optical tracking system (ELITE) (5, 13). This system has been previously described for respiratory use (13); however, we used an extended marker configuration with 86 markers rather than 32 (5) to improve volume accuracy and to delimit anatomically the specific rib cage compartments. Figure 3 shows the anatomic placement of the markers, and Fig. 4 illustrates the construction of the volume compartments. The markers were tracked in three dimensions by four videocameras: two in front of the subject and two behind. Each set of cameras was aligned vertically: one near the floor and the other near the ceiling. Volumes for each compartment were calculated by constructing a triangulation over the surface and then using Gauss's theorem to convert the volume integral to an integral over this surface, as described previously (5). The ELITE system calculates absolute volumes, and we used the absolute volume of each

Table 1. *Anthropometric data*

Subject	Age, yr	Height, m	Weight, kg	FRC, liters	VC, liters	TLC, liters
CK	31	1.80	83	3.2 (84)	5.2 (102)	8.0 (114)
II	32	1.84	94	3.5 (100)	5.7 (102)	7.7 (103)
PG	33	1.70	77	3.5 (108)	5.5 (116)	6.9 (106)
SC	38	1.78	78	4.1 (109)	6.0 (117)	8.2 (117)
SY	38	1.68	60	2.9 (97)	4.7 (129)	6.3 (122)
Mean ± SD	34.4 ± 3.4	1.76 ± 0.07	78.4 ± 12.3	3.4 (100) ± 0.4 (10)	5.4 (113) ± 0.5 (11)	7.4 (112) ± 0.8 (8)

FRC, functional residual capacity; VC, vital capacity; TLC, total lung capacity. Values in parentheses represent percent predicted.

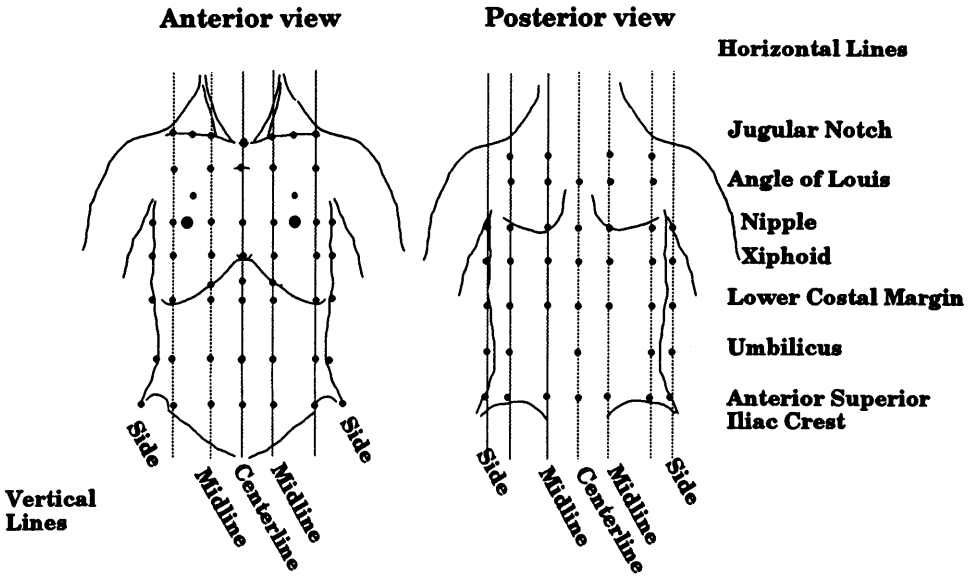

Fig. 3. Placement of passive reflective markers on chest wall: 7 horizontal rows of 12 markers with additional markers added for anatomic detail or uniform marker density for a total of 86 markers.

compartment at functional residual capacity (FRC) as the reference volume. Volumes are reported in absolute numbers or as deviations from FRC expressed as percent vital capacity for that compartment.

We defined the abdominal compartment as extending caudally from the lower rib cage to the level of the anterior superior iliac crest and used the surface markers to calculate its volume (Vab). Thus the chest wall volume $V_{CW} = V_{rc,p} + V_{rc,a} + V_{ab}$, and changes in V_L can be calculated as

$$\Delta V_L = \Delta V_{rc,p} + \Delta V_{rc,a} + \Delta V_{ab}$$

This assumes that blood shifts to and from the trunk and gas compression can be ignored. We validated this measure of changes in V_L by simultaneously measuring volume changes with a water displacement spirometer with a CO_2 absorber during the 20 s of data collection. Comparisons were done with spirometer volumes adjusted to BTPS and corrected for O_2 consumption by removing the mean slope of the spirometer drift. We also validated the system by summing $\Delta V_{rc,p}$, $\Delta V_{rc,a}$, and ΔV_{ab} during isovolume maneuvers and during phrenic twitches against a closed airway when $\Delta V_L = 0$. Data

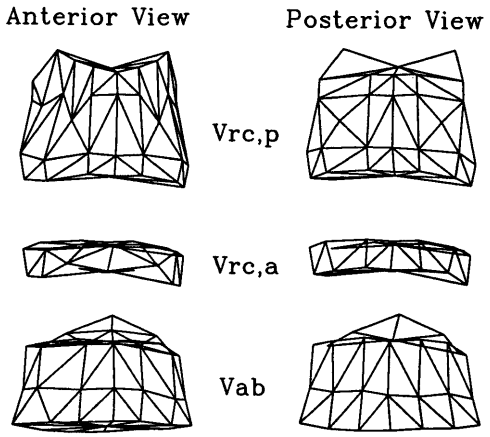

Fig. 4. Division of chest wall into volume compartments. RCp is separated from RCa at level of xiphisternum, caudal border of Rca is at costal margin anteriorly down from xiphisternum and straight across posteriorly at most caudal level of lower rib cage. Vab, volume of abdomen.

collection was carried out at 100 Hz. Length of collection was limited to 20 s by system overload, which generally occurred with 86 markers after 25 s of collection because of hardware limitations. Volume validations have previously been presented with this system and marker configuration, along with a sensitivity analysis, which assess accuracy as a function of marker number and position (5).

Pressure measurements. Pes and Pga were measured using catheter-balloon systems connected to pressure transducers (Validyne MP 45, ± 100 cmH_2O) and recorded digitally onto the IBM-compatible PC, which was also used for the marker positions via the ELITE system. Mouth pressure (Pm) was also recorded via a pressure transducer (Validyne MP 45, ± 100 cmH_2O) attached to the mouthpiece.

Measurement of rib cage distortability and restoring pressures. Relaxation characteristics were established for the chest wall by having subjects breathe in to total lung capacity and then relax and breathe out through a high resistance to FRC. Relaxation maneuvers were repeated until curves were reproducible, Pm finished at zero, and Pdi was zero throughout. A plot of Vrc,p vs. Vrc,a during relaxation defined the undistorted rib cage configuration.

Distortions were measured during bilateral transcutaneous phrenic stimulation with submaximal single twitches and supramaximal single and double twitches. Twitches were 1 ms in duration and 50 ms apart for double twitches and were repeated 10 times at 2-s intervals during breath holding at FRC with the glottis closed. Electrical activity of the diaphragm was monitored from surface electrodes in the sixth and seventh intercostal spaces on each side. The mass action potentials for any given stimulus mode were highly reproducible and for supramaximal stimuli were independent of current. Distortability and P_{link} were calculated as described above.

Data analysis. Rib cage distortion and P_{link} were calculated at each level of exercise from average breaths created for each subject by linear stretch, so breaths of different duration could be combined. Overall the breaths combined were very uniform, requiring $<10\%$ stretching, except in one subject (*PG*) at the lowest level of exercise. We calculated average distortion and range of distortion over these average breaths as well as the corresponding values of P_{link}. Pdi was measured directly as Pga − Pes. Knowing P_{link}, Pes, and Prc,p allowed us to calculate Prcm as the only unknown in *Eq. 4*.

RESULTS

Volume comparison with spirometry. Figure 5 shows the worst comparison between the chest wall volume changes calculated from surface markers using the ELITE system and water displacement spirometry at the highest level of exercise (70% $\dot{W}$max). The worst coefficient of variation of the two signals was 4%. The mean regression coefficient between the two was 0.97 ± 0.04 (SD) (range 0.93–1.04), with a mean intercept of 0.01 ± 0.04 (SD) liter (range −0.05 to +0.06l) for all subjects at the highest level of exercise (Table 2).

Volume changes with phrenic twitch (closed glottis). The summed value of ΔVrc,p, ΔVrc,a, and ΔVab during twitch diaphragm contractions was +0.059 ± 0.12l (SD) liter (n = 104) with no relation to twitch Pdi (r^2 for regression = 0.01). Vab increased and Vrc,p decreased by approximately equal amounts in each twitch by up to 0.4 liter at a ΔPdi of 25 cmH_2O. Vrc,a changed very little: the maximum increase was 0.015 liter, and the maximum decrease was 0.010 liter. Regression relations were $\Delta Vrc,p = -0.013\Delta Pdi - 0.01$ (r^2 = 0.65), $\Delta Vab = 0.012\Delta Pdi + 0.046$ (r^2 = 0.69), and $\Delta Vrc,a = 0.002\Delta Pdi - 0.007$ (r^2 = 0.05), using all the twitch data for all subjects.

Rib cage pressure-volume characteristics. The pressure-volume relations of the rib cage compartments during relaxation and phrenic twitches are shown in Fig. 6. Relaxation was from total lung capacity to FRC, and twitches were also performed at FRC; linear extrapolation was performed for volumes below FRC. The dynamic compliances during phrenic stimulation of RCp and RCA (C′rc,p and C′rc,a) were less than their static compliances (Crc,p and Crc,a), and ΔVrc,a during phrenic stimulation was almost zero. These compliances were calculated as ΔVrc,p/ΔPes and ΔVrc,a/ΔPga, respectively, during relaxation and phrenic twitches and are shown in Table 3. Crc,a is roughly one-half of Crc,p. C′rc,p is only 21% of Crc,p, and C′rc,a is effectively zero. This indicates that compartmental compliance decreases greatly if the rib cage is distorted; in fact, C′rc = C′rc,p + C′rc,a is 10% of Crc = Crc,p + Crc,a.

Table 2. *Linear regression parameters of ELITE measurement of chest wall volume changes with respect to volume changes measured by water displacement spirometer*

Subject	Intercept, liter	Slope	r^2	Coeff. of Variation, %
SC	−0.05	0.96	0.99	4.0
CK	0.03	0.95	0.96	2.9
II	0.03	1.04	0.98	0.9
PG	−0.01	0.95	0.96	2.0
SY	0.06	0.93	0.98	0.4
Mean ± SD	0.01 ± 0.04	0.97 ± 0.04	0.97 ± 0.01	2.0 ± 1.6

Values are corrected for BTPS. Coeff., coefficient.

Rib cage distortions and resulting restoring pressures. Because Pdi is proportional to the pressure producing distortion (9), a plot of percent distortion vs. Pdi defines rib cage distortability in each of the five subjects during phrenic stimulation (Fig. 7). With increasing distorting pressure (Pdi), the percent rib cage distortion increased nonlinearly, with less distortion at higher pressures in three subjects, more in one subject, and no change in another. Distortions of up to 2.5% were achieved for Pdi of up to 30 cmH_2O.

Figure 8 shows restoring pressures (P_{link}) plotted against the rib cage distortions producing them during phrenic stimulation for the five subjects. The relation was generally nonlinear, with greater restoring pressure with increasing distortion in three subjects, slightly decreasing in one subject, and constant in another subject. Restoring pressures of up to 15 cmH_2O were developed with distortions of up to 2.5%.

Figure 9 shows rib cage restoring pressures plotted against Pdi for the five subjects during phrenic stimulation. This describes how the pressure generating the distortion is transduced via distortion into a restoring pressure. The relation was linear in all cases, with mean slope of 0.40 ± 0.055 (SD) for the different subjects. This is as expected, inasmuch as most of the ΔPes during a twitch is due to P_{link}; the change in Prc,p was small in comparison. Thus $P_{link} \approx -\Delta Pes$, Pdi =

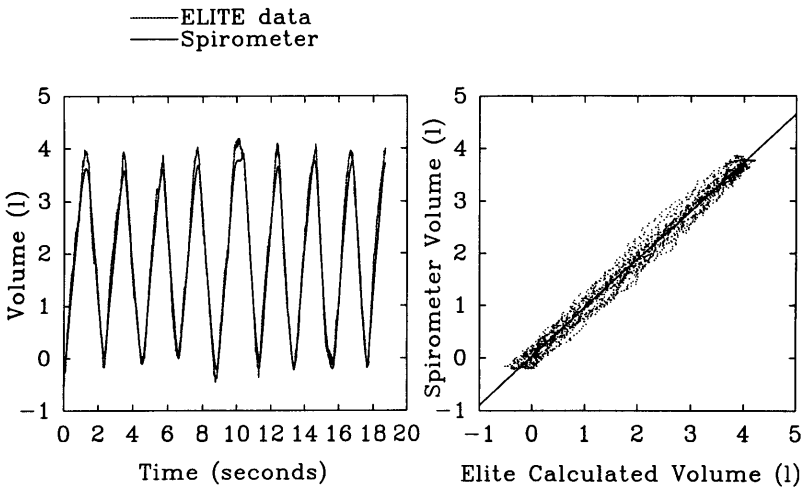

Fig. 5. Worst example of correspondence between chest wall volume change calculated from surface markers (SM) compared with water displacement spirometry (WDS) at highest level of exercise. Regression equation is as follows: SM = 0.96WDS − 0.05, where values are in liters, coefficient of variation = 4%, and r^2 = 0.994.

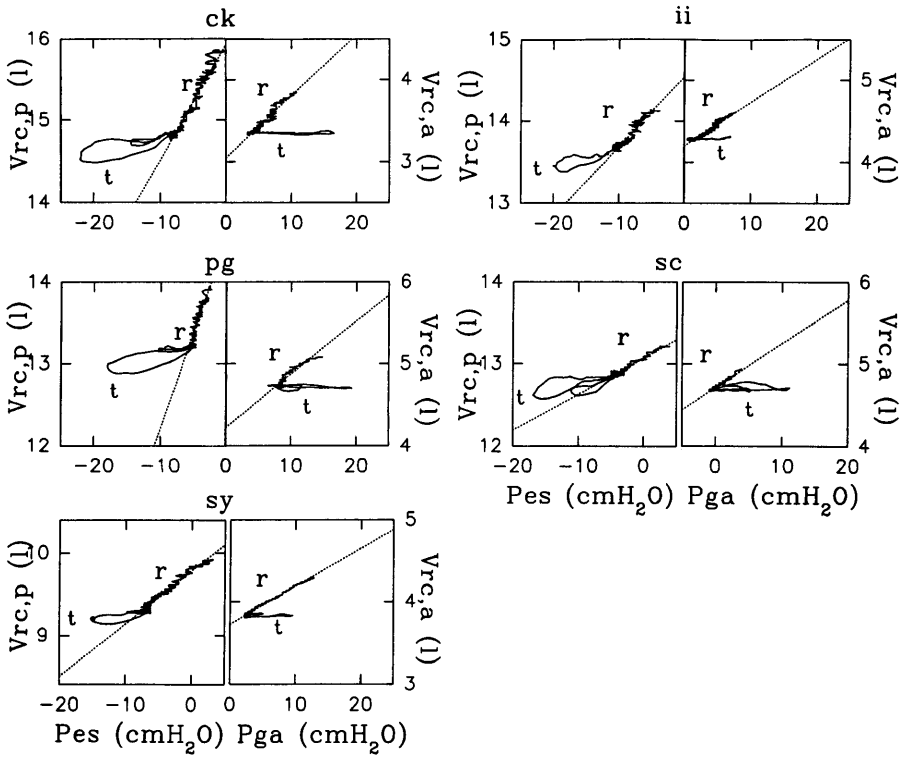

Fig. 6. Pressure-volume characteristics of rib cage compartments of 5 subjects during relaxation (r) and phrenic stimulation (t). Phrenic stimulation was done at functional residual capacity with glottis closed.

ΔPga − ΔPes, and ΔPes/Pdi ≈ 0.5, so we expected P_{link}/Pdi ≈ 0.5, as shown in Fig. 9.

Figure 10 shows the average time course of the raw data, i.e., the signals that were directly observed (Pes, Pga, Pdi, Vrc,p, Vrc,a, and Vab), for all the subjects during quiet breathing and exercise.

Important points that we will elaborate here and later (3) are as follows: *1*) end-expiratory rib cage volume did not change, whereas end-inspiratory rib cage volume progressively increased from quiet breathing to exercise at 70% Wmax; *2*) end-inspiratory abdominal displacement changed little, whereas end-expiratory abdominal displacement progressively diminished from quiet breathing to exercise at 70% Wmax; *3*) Pga rose throughout inspiration during quiet breathing, but during most of inspiration during exercise, even at 0% Wmax, it fell, tending to parallel the fall in Pes; *4*) the slope Pdi/T_I (where T_I is inspiratory time) was steeper during quiet breathing than during all levels of exercise during most of inspiration; *5*) at all levels of exercise, Pdi was finite at the onset of inspiration (probably because of passive stretching), and this increased progressively with Wmax. Thus, although active Pdi at end inspiration increased from ~10 cmH_20 during quiet breathing to ~20 cmH_20 at 70% Wmax, ΔPdi during inspiration was lower during exercise than during quiet breathing, except at 70% Wmax.

During exercise a pattern of distortion different from that in phrenic stimulation was observed. Figure 11 shows data plotting Vrc,p vs. Vrc,a during quiet breathing and at each exercise level for the average breath. The dotted lines are at iso-P_{link} values of ±2.5, ±5, and ±10 cmH_2O and are parallel to the relaxation line for each subject. These data illustrate that in all subjects the rib cage always moved parallel to its relaxation line with different levels of exercise, and there was very little distortion. On average, distortion was constant throughout the respiratory cycle at any level of exercise. However, the Vrc,p vs. Vrc,a trace tended to form a loop, which appeared to increase in width as exercise level increased. Consequently, we measured mean rib cage distortion as the parallel shift of the trace and

Table 3. *Compartmental rib cage compliances during relaxation and phrenic stimulation*

	Relaxation		Phrenic Twitch		Ratio	
Subject	Crc,p	Crc,a	C′rc,p	C′rc,a	C′rc,p/Crc,p	C′rc,a/Crc,a
CK	0.140	0.075	0.021	0.000	0.150	−0.002
II	0.079	0.053	0.021	0.004	0.265	0.068
PG	0.232	0.065	0.018	−0.003	0.077	−0.039
SC	0.044	0.053	0.016	0.002	0.365	0.041
SY	0.064	0.046	0.012	0.000	0.189	−0.022
Mean ± SD	0.112 ± 0.076	0.059 ± 0.012	0.018 ± 0.037	0.000 ± 0.002	0.209 ± 0.111	0.009 ± 0.044

Crc,p and Crc,a, pulmonary and abdominal rib cage compliances during relaxation; C′rc,p and C′rc,a, pulmonary and abdominal rib cage compliances during phrenic stimulation. Compliance values are l/cmH_2O.

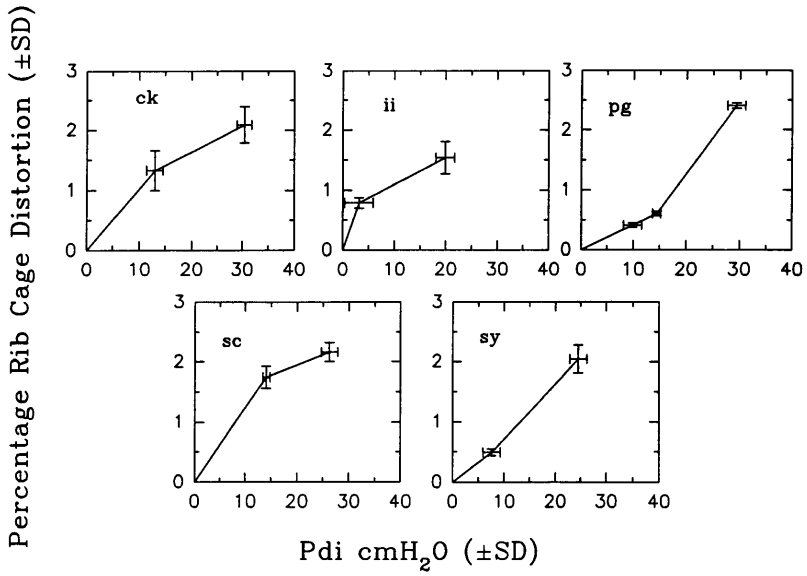

Fig. 7. Individual subject rib cage distortions plotted against transdiaphragmatic pressure (Pdi), which is proportional to distorting pressure difference. Subjects' initials are in *top left* of each panel.

range of distortion as the width of the loop as a way of quantifying the change in distortion during a breath. These data are shown in detail in Table 4. Mean distortion and P_{link} were less during quiet breathing than during exercise. Mean rib cage distortion remained <0.5%, with no consistent individual changes. Mean P_{link} during exercise remained nearly constant at an average value of −2.0 cmH_2O, with no consistent change with exercise level. Range of distortion over a breath increased linearly from 0.36% at quiet breathing to 1.00% at 70% Wmax. The corresponding range of P_{link} over a breath increased linearly from 1.34 to 3.99 cmH_2O. As a percentage of the pressure generated by the inspiratory rib cage muscles at end inspiration, this was 20 ± 3.9% (SE) during quiet breathing and 13 ± 4.1% (SE) at 70% Wmax. The maximum contribution of P_{link} was at 0% Wmax, when it was 27 ± 6.5% (SE) of the peak values of the pressures developed by the nondiaphragmatic inspiratory muscles.

Relationship between diaphragm-apposed rib cage and abdominal pressure. Figure 12 shows that Vrc,a changed less with Pab during quiet breathing than during relaxation. It also shows that Vrc,a changed less with Vab during quiet breathing than during relaxation; thus there was distortion away from the Vrc,a-Vab relaxation configuration. This is in contrast to the results of Ward et al. (31), who found that the slope ΔVrc,a/ΔPab was greater during quiet breathing than during relaxation, as would be expected if Pab and the insertional component of Pdi (*x*Pdi) were the only agencies acting on RCa during quiet breathing. Evidently, one or more additional agencies diminish the combined effect of Pab and *x*Pdi on RCa.

DISCUSSION

Using a two-compartment model to describe the rib cage (31) and calculating compartmental volumes from surface markers (5, 13), we have found that the human rib cage distorts very little in exercise up to 70% Wmax, averaging about −0.3% (Table 4), leading to restoring pressures of ~17% of those generated by the nondiaphragmatic inspiratory muscles at the highest level of exercise. During respiration the range of distortions

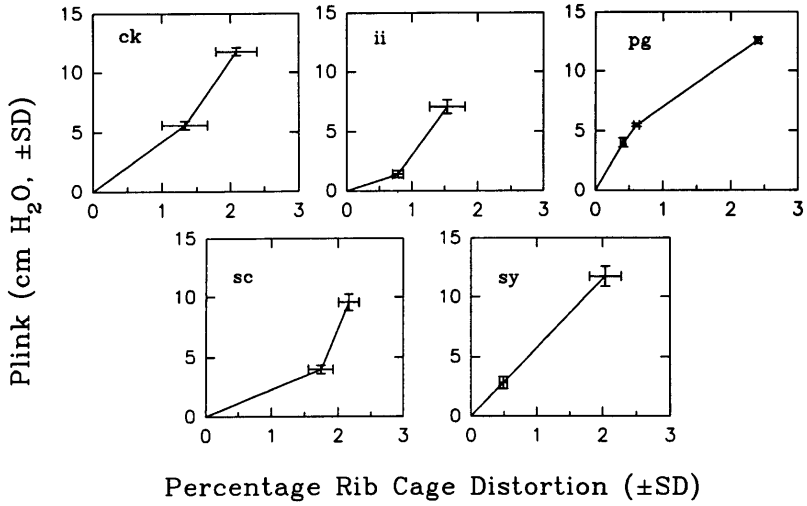

Fig. 8. Rib cage stiffness for each subject shown as restoring pressure generated by distortion against distortion causing it.

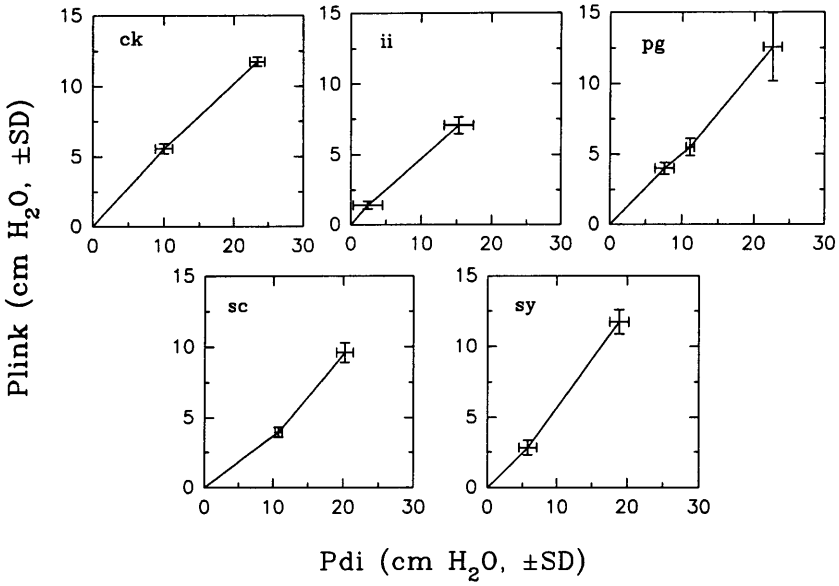

Fig. 9. Coupling between restoring and distorting pressures: Pdi is proportional to distorting pressure, and P_{link} is restoring pressure resulting from rib cage distortion.

increased linearly with exercise level from 0.36 to 1.00%, but the resulting restoring pressure expressed as a percentage of the pressure generated by the rib cage muscles remained roughly constant: 20% during quiet breathing and 13% at 70% Wmax. In comparison, distortions during phrenic stimulation, with Pdi of up to 30 cmH_2O, were substantial (Fig. 7) and resulted in restoring pressures of >10 cmH_2O in four of five subjects. The slope of the volume-pressure relaxation line is the compliance of RCp or Crc,p (Fig. 6). During phrenic stimulation, this slope C′rc,p was only 21% of Crc,p, and C′rc,a was effectively zero. The mechanical linkage between RCp and RCa markedly stiffens the whole rib cage when it is distorted. Indeed, we found that rib cage compliance during phrenic stimulation was only 10% of that during relaxation, confirming the work of Chihara et al. (9). Although this enhances the inspiratory function of the diaphragm, defined as the fraction of Pdi that is converted to a fall of Ppl (9), it means that a substantial fraction of respiratory muscle force may be used to distort the rib cage rather than to change the volume of the respiratory system.

Critique of model. A detailed critique of the model has been published (31). Here we restrict ourselves to those points that are particularly relevant for exercise. In the model, RCp and RCa are divided at the transverse level of the xiphisternum. This is the approximate upper boundary of the diaphragm-apposed part of the rib

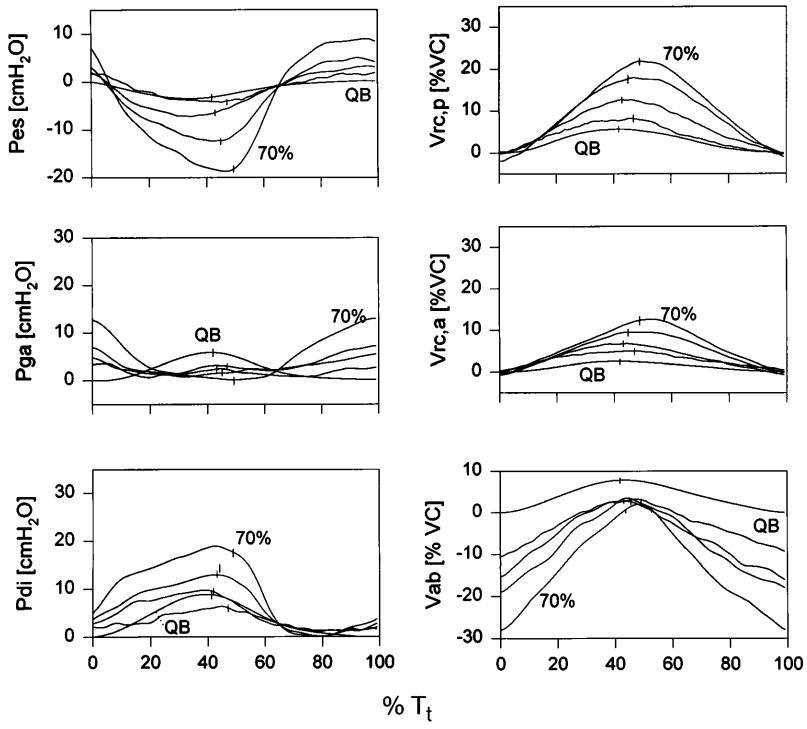

Fig. 10. Mean raw data for pressures and volumes over all subjects during quiet breathing (QB) and at all levels of exercise. Pga, gastric pressure. TT, respiratory cycle duration.

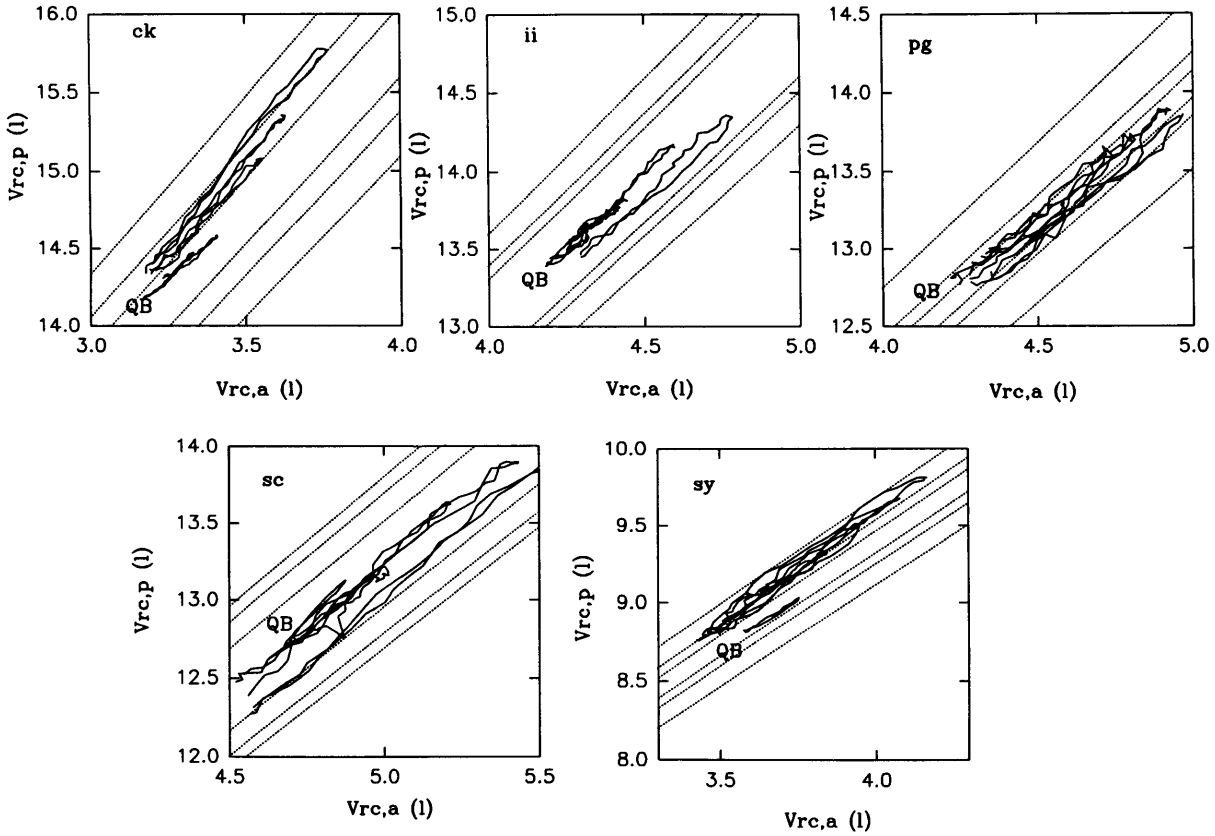

Fig. 11. Plots of Vrc,p vs. Vrc,a for all subjects during quiet breathing and at all levels of exercise. Dotted lines, iso-P_{link} values of ±2.5, ±5, and ±10 cmH_2O.

cage. The sixth rib attaches to the sternum just above this level, and the ventral extremity of the seventh rib is below this level. The parasternal and scalene muscles insert only on the ribs contained by RCp. The external intercostals, which are also inspiratory, are recruited from above downward during exercise and thus act exclusively on RCp, except at higher levels of exercise, when they also act on RCa. Our estimates of Prcm only include the pressures developed on RCp. They do not include pressures developed by the nondiaphragmatic inspiratory muscles on RCa. Estimates of expiratory Prcm are valid only for RCp. Inasmuch as internal intercostals are usually recruited from below upward during exercise, there may have been considerable expiratory rib cage muscle action on RCa that we did not measure.

The diaphragm, which inserts only on ribs 7–12, acts directly only on the ribs contained in RCa. However, a slip of the diaphragm originates from the lower end of the sternum and thus has a direct effect on RCp. Because this attachment comprises only a small percentage of all the diaphragmatic fibers, we believe that the direct action of the diaphragm on RCp is small and that most of the diaphragm's action on RCp is mediated through the rib cage distortions that we measured during phrenic stimulation. Although we ignore the direct action of the diaphragm on RCp, this assumption needs to be borne in mind as a potential source of error in the present analysis. However, whatever the resulting error, it presumably diminishes as exercise level increases. Interestingly, we found that active $\dot{P}di$ decreased from quiet breathing to exercise at 0% Wmax and only doubled from quiet breathing to exercise at 70% Wmax. Prcm, in contrast, increased on average 4.5-fold from quiet breathing to 70% Wmax (see Ref. 5 for details on rib cage and abdominal muscle contribution).

During exercise, tidal volume increases (15, 29), diaphragm excursion increases (15, 16, 30), and the upper boundary of the diaphragm-apposed rib cage may descend (22, 25). Thus the boundary between RCp and RCa is continuously changing. This clearly affects the dynamics of the lower rib cage, the boundary of which in the present model was fixed. It has smaller effects on the upper rib cage, because even at very low V_L the zone of apposition does not extend far above the xiphisternum (22). In this presentation we ignore these sources of error. Fortuitously, we found that rib cage distortions were small and varied little throughout a breath. The sources of error do not affect this observation, which must mean that the net pressures acting on both rib cage compartments were not very different. This would act to minimize the errors. Furthermore, to the extent that abdominal displacement is the principal determinant of the upper boundary of the area of apposition, the similarity of this displacement at end inspiration during quiet breathing and at all levels of exercise suggests that its caudal excursion during inspiration was not greatly affected by exercise. We

Table 4. *Rib cage distortions and restoring pressures during exercise*

Subjects, Conditions	Distortion, %		P_{link}, cmH_2O		Slope/ Relaxation
	Mean	Range	Mean	Range	
CK					
QB	0.02	0.21	0.08	0.88	0.88
0% $\dot{W}$max	0.05	0.37	0.20	1.54	0.75
30% $\dot{W}$max	−0.39	0.33	−1.65	1.38	1.00
50% $\dot{W}$max	−0.59	0.37	−2.48	1.54	1.06
70% $\dot{W}$max	−0.89	0.56	−3.72	2.37	1.14
II					
QB	−0.20	0.42	−0.36	0.74	1.12
0% $\dot{W}$max	−0.12	0.50	−0.22	0.90	0.97
30% $\dot{W}$max	−0.22	0.62	−0.39	1.10	1.03
50% $\dot{W}$max	−0.60	0.86	−1.25	2.89	1.12
70% $\dot{W}$max	−0.11	1.20	−0.19	2.13	1.05
PG					
QB	−0.05	0.43	−0.25	2.22	1.02
0% $\dot{W}$max	−0.52	0.67	−2.71	3.53	0.94
30% $\dot{W}$max	−0.29	0.81	−1.52	4.26	0.96
50% $\dot{W}$max	0.01	0.85	0.07	4.44	1.09
70% $\dot{W}$max	0.14	1.00	0.72	5.22	0.91
SC					
QB	−0.23	0.45	−0.58	1.15	1.37
0% $\dot{W}$max	0.19	1.16	0.47	2.93	0.93
30% $\dot{W}$max	−0.10	0.58	−0.24	1.47	1.01
50% $\dot{W}$max	0.06	0.89	0.15	2.25	0.99
70% $\dot{W}$max	0.80	0.83	2.02	2.09	0.99
SY					
QB	0.01	0.30	0.06	1.71	0.90
0% $\dot{W}$max	−1.25	0.85	−7.19	4.87	0.90
30% $\dot{W}$max	−1.21	0.93	−6.98	5.32	1.13
50% $\dot{W}$max	−1.16	1.21	−6.70	6.91	1.12
70% $\dot{W}$max	−1.35	1.41	−7.79	8.08	1.07
Mean ± SE					
QB	−0.09 ± 0.04	0.36 ± 0.04	−0.07 ± 0.24	1.34 ± 0.28	1.06 ± 0.09
0% $\dot{W}$max	−0.33 ± 0.26	0.71 ± 0.14	−1.89 ± 1.44	2.75 ± 0.57	0.90 ± 0.04
30% $\dot{W}$max	−0.44 ± 0.20	0.65 ± 0.10	−2.16 ± 1.24	2.71 ± 0.87	1.03 ± 0.03
50% $\dot{W}$max	−0.46 ± 0.22	0.84 ± 0.13	−2.04 ± 1.26	3.60 ± 0.95	1.08 ± 0.02
70% $\dot{W}$max	−0.28 ± 0.38	1.00 ± 0.15	−1.79 ± 1.78	3.99 ± 1.18	1.03 ± 0.04

P_{link}, restoring pressure (see *Glossary*); QB, quiet breathing; $\dot{W}$max, maximum exercise workload; slope/relaxation, regression slope for exercise level divided by that during relaxation for relationship between pulmonary and abdominal rib cage volume.

believe that the error introduced by a changing boundary of the upper limit of the area of apposition on the dynamics of RCa and RCp is small and that it can be ignored.

The model used here does not deal with intracompartmental distortions but only distortions between compartments. A surprising finding of this study is that volume distortion of the rib cage is very small in exercise; this contrasts with previous investigations in normal adults, in which significant cross-sectional shape or area changes have been found during voluntarily and involuntarily increased ventilation (1, 11, 22, 27, 28). Rib cage distortion in exercise has not been previously studied, although it has been shown that the rib cage is not on its volume-pressure relaxation characteristic (14–16). It is not obvious how to incorporate intracompartmental distortion into the present analysis, and available work on more detailed models of the rib cage is generally incomplete in terms of incorporating all the relevant muscular anatomy (e.g., omission of the diaphragm) and the mechanical properties of component tissues (bones, muscles, and connective tissue) (10, 17). Incorporating these variables leads to considerable complexity in producing a truly rigorous analysis. By employing simplifying assumptions, we are able to estimate rib cage distortability, restoring forces, and the Prcm instantaneously during inspiration and expiration. This has not been possible previously.

Critique of methods. Surface markers were used for compartmental volume calculation. This is inevitably imprecise, in that there can be movement of skin relative to the underlying bone structure during increased ventilation. We carefully observed marker movements relative to anatomic features and found a maximum of ±1.5 cm of marker displacement relative to the lower costal margin in the anterior auxiliary lines in our subjects. Movement at other points on the intercompartmental boundaries was much less and became negligible at the bottom of the sternum, lateral margins, and posteriorly. This could lead to errors in compartmental volume changes of RCa vis-à-vis the abdomen. The errors relative to the absolute volume of the compartments (~4 liters for RCa and ~12 liters for the abdomen) were <10% for Vrc,a and <2.5% for Vab. We neglected these errors.

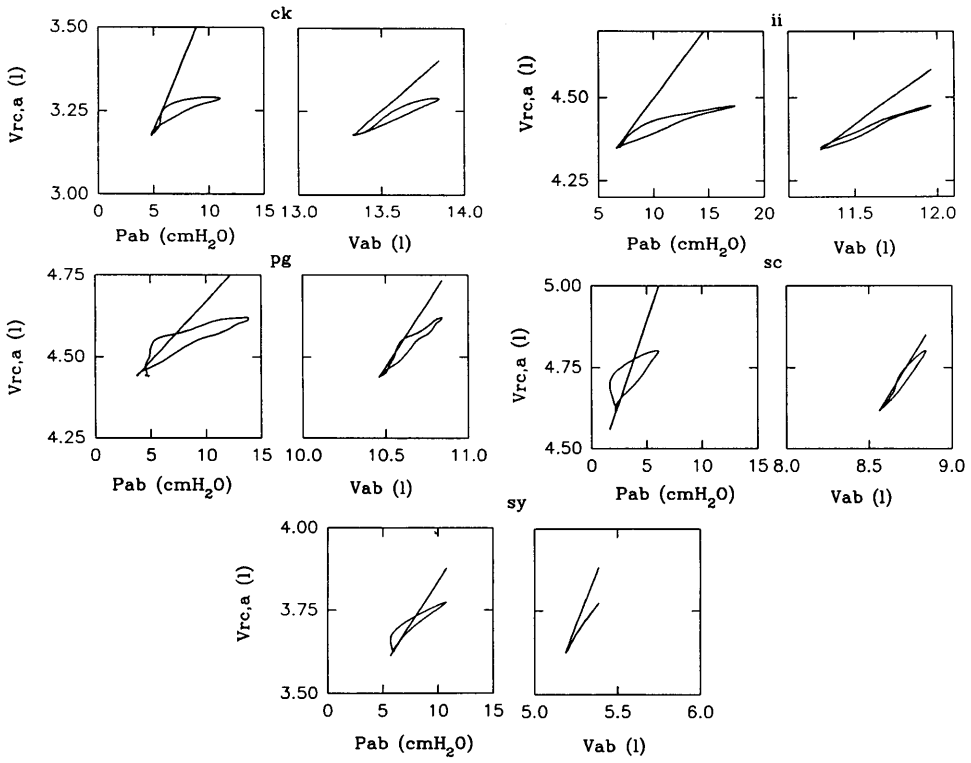

Fig. 12. Details of lower rib cage (Vrc,a) behavior for all subjects (initials above each pair of panels). In each pair, *left panel* shows pressure-volume relationship for Vrc,a for relaxation (straight line) and quiet breathing (loop, time course is counterclockwise), and *right panel* shows Vrc,a vs. Vab relation for relaxation (straight line) and quiet breathing (loop, time course is counterclockwise).

Data were gathered after 3 min at each level of exercise, a time sufficient for normal subjects to reach a steady state (8). However, the subjects' posture with arms supported away from the body was not that normally used during cycling. We do not know whether this altered rib cage elastic properties, and strictly speaking our results apply only to the type of exercise performed in this study. We did not observe entrainment of respiratory rate to cycling rate in this study; when this occurs, as in swimming, results might be different. Finally, although changes in blood flow, autonomic activity, and so forth during exercise might conceivably have altered relaxation configurations, we, like others (14, 16, 21, 27, 28), made no attempt to control these variables.

Rib cage compliance and distortion. We found that, during relaxation, Crc,p was approximately twice Crc,a: 0.112 and 0.059 l/cmH_2O, respectively. This is probably accounted for by the larger volume of Crc,p. However, during bilateral phrenic twitch, C′rc,p declined to 21% of its previous value and C′rc,a was effectively zero, confirming the findings of Chihara et al. (9), who used cross-sectional areas to represent volume changes. Thus the compliance of the rib cage during distortion is reduced to 10% of its undistorted value, at least in normal subjects. This implies that when the action is inflationary on one part of the rib cage and deflationary on the other part, the net effect will generate only 10% of the volume change that would occur if the agencies acting on the rib cage were properly coordinated to move it along its relaxation configuration. This provides an excellent teleological reason for the small amount of distortion we found during exercise; as a result, restoring pressures were usually small relative to inspiratory rib cage muscle pressure generation.

Implications of lack of rib cage distortion in exercise. The small amount of observed distortion during exercise requires that the muscles acting on the upper and lower rib cages be precisely coordinated throughout each breath to avoid a pressure difference that would cause distortion. From the pressure balance equations on RCp and RCa derived from the model shown in Fig. 1, we can write the condition for no rib cage distortion

$$\mathrm{Prc,p} = \mathrm{Prc,a}$$

When this condition is fulfilled, P_{link} is zero, and from *Eq. 4*

$$\begin{aligned} \mathrm{Prc,p} &= \mathrm{Prcm} + \mathrm{Ppl} \\ \mathrm{Prc,a} &= x\mathrm{Pdi} + \mathrm{Pab} - y\mathrm{Pabm} \end{aligned} \qquad (5)$$

Therefore

$$\mathrm{Prcm} + \mathrm{Ppl} = x\mathrm{Pdi} + \mathrm{Pab} - y\mathrm{Pabm}$$

rearranging we find that the condition for no distortion is

$$\mathrm{Prcm} = (x + 1)\mathrm{Pdi} - y\mathrm{Pabm}$$

This equation states that the pressures developed by the rib cage muscles (Pcrm), which increase during inspiration, must equal the sum of Pdi plus its insertional component (xPdi), which also increases during inspiration, less that component of the pressure developed by the abdominal muscles (Pabm), which acts to deflate RCa and decreases during inspiration. Accord-

ing to the model, this relation must be kept between the muscle pressures in order for there to be no distortion. Thus, to account for the minimal distortion we observed in this investigation, we predict that this equation is applicable. How this is done is the subject of another article (3), which discusses the muscle pressures and their coordination.

Behavior of the rib cage during quiet breathing. As shown in the plot of Fig. 12, Vrc,a vs. Pab during quiet breathing is to the right of the relaxation line for all five subjects, indicating net expiratory pressures on the lower rib cage during expiration and, more surprisingly, most of inspiration compared with relaxation. These expiratory pressures could not have come from expiratory rib cage muscles, inasmuch as these are not active in quiet breathing. Although there may be tonic activity of abdominal muscles during relaxation and quiet breathing, any phasic activity is limited essentially to expiration and is small (7). The departures from the relaxation curve that we observed were present through the respiratory cycle. Similarly, during quiet breathing the volume of the abdominal compartment relative to the lower rib cage volume increased more than during relaxation (Fig. 12). This is probably due to the action of the diaphragm in quiet breathing compared with relaxation, when it is passive (18). This increase in abdominal compartmental volume relative to lower rib cage volume during quiet breathing and the concomitant increase in Pab will passively stretch the abdominal muscles more than during relaxation. In fact, during quiet breathing the normal increase in Pab, particularly in the upright posture, must passively stretch the abdominal muscles. Inasmuch as the rib cage is indifferent as to whether the force applied to it is active or passive, we believe that passive tension in the abdominal muscles exerts an important deflationary action on RCa during tidal inspiration. This effect is included in *Eq. 5*, where the first two terms on the right-hand side represent the actions of the diaphragm and Pab, whereas the third term represents the pressure exerted by passive stretching of the abdominal muscles. This effect increases monotonically with Pab throughout inspiration. This contrasts with the situation in exercise when abdominal muscles actively contract in expiration. During the subsequent inspiration the abdominal muscles gradually relax (3), and active tension is replaced by passive tension. The net effect is for the relaxation during inspiration to have a progressive inflationary action on the rib cage throughout inspiration, whereas during quiet breathing the effect is progressively deflationary. This action of abdominal muscles during quiet breathing has not previously been identified.

Other measures of distortion. Chest wall shape distortion has been reported by using cross-sectional diameter ratios (circular vs. elliptical configurations) and has been associated with the action of particular muscle groups during inspiratory or expiratory efforts (11, 21, 23, 24, 27). There have been few attempts to quantify the consequences of these observed distortions in terms of forces or volume effects. One study concluded that rib cage distortion reduced tidal volume in infants and rats by one-half (24), in contrast to our result in adult humans of very little volume reduction. This probably reflects species differences and the effect of maturation on rib cage distortability.

Rib cage distortions measured by Ward et al. (31) during quiet breathing were greater than those measured by us, and they concluded that ~50% of the fall in Ppl over the costal surface of the lung was contributed by P_{link}. They also reported, in contrast to our findings, that $\Delta Vrc,a/\Delta Pab$ was greater during quiet breathing than during relaxation. This difference could be due to the fact that our subjects were seated on a cycle ergometer and so had a different posture. It is likely, however, that we estimated smaller distortions because we measured volume distortion, whereas Ward et al. measured shape distortion. The latter appears to be greater than volume distortion, and this may have exaggerated the estimate of P_{link} reported by Ward et al., who assumed that the shape distortion that they measured reflected volume distortion. Under the circumstances, deducing volume from a single dimension would lead to a systematic overestimation of Vrc,a, explaining their finding of an increased $\Delta Vrc,a/\Delta Pab$ during quiet breathing. In the present analysis we measured the pressures producing volume distortions (Pdi) and the restoring pressures (P_{link}). The pressures producing shape distortion within RCp and RCa and their resulting restoring forces are unknown.

Distortion of the rib cage/abdomen relative to their relaxation configuration has been analyzed by Goldman, Grimby, and Mead (14, 16), who showed that these deformations were substantial. However, the pressure cost of rib cage/abdomen deformation is sufficiently small that it can be neglected (4).

To conclude, this investigation demonstrates that the diaphragm, rib cage, and abdominal muscles are coordinated during exercise so that rib cage distortions, although measurable, are minimized. The pressure cost of these distortions is only a small percentage of the pressures applied to RCp during exercise. The net pressure acting on the two rib cage compartments must therefore be closely similar. Inasmuch as the abdominal rib cage is exposed to a large positive Pab at end expiration in exercise, this must be counterbalanced by a strong expiratory action resulting from active contraction of expiratory muscles. We believe that the insertional component of abdominal muscles is a major contributor to this expiratory action and thus plays a key role in minimizing rib cage distortion. This minimization prevents a marked reduction in rib cage compliance, which would substantially increase elastic work of breathing. Finally, we believe that passive stretching of abdominal muscle is important in preventing rib cage distortion during quiet breathing. In doing so, it plays a previously unrecognized role in displacing the dynamic Pab-rib cage volume curve to the right of the relaxation line, which more than compensates for the combined inflationary action of the Pab insertional component of Pdi.

This work was supported by the Medical Research Council of Canada, Respiratory Health Network of Centre of Excellence, Montréal Chest Institute, Allen and Hanburys Thoracic Society of Australia and New Zealand Fellowship, J. T. Costello Memorial Research Fund, and Fondazione Pro Juventute, Italy, Telethon Italy.

Address for reprint requests: P. T. Macklem, Montréal Chest Institute, 3650 St. Urbain, Montreal, Quebec, Canada H2X 2P4.

Received 24 July 1996; accepted in final form 17 April 1997.

REFERENCES

1. **Agostoni, E., P. Mognoni, G. Torri, and G. Miserocchi.** Forces deforming the rib cage. *Respir. Physiol*. 2: 105–117, 1966.
2. **Agostoni, E., and H. Rahn.** Abdominal and thoracic pressures at different lung volumes. *J. Appl. Physiol*. 15: 1087–1092, 1960.
3. **Aliverti, A., S. J. Cala, R. Duranti, G. Ferrigno, C. M. Kenyon, A. Pedotti, S. G. Scano, P. Sliwinski, P. T. Macklem, and S. Yan.** Human respiratory muscle actions and control during exercise. *J. Appl. Physiol*. 83: 1256–1269, 1997.
4. **Boynton, B. R., G. M. Barnas, J. T. Dadmun, and J. J. Fredberg.** Mechanical coupling of the rib cage, abdomen, and diaphragm through their area of apposition. *J. Appl. Physiol*. 70: 1235–1244, 1991.
5. **Cala, S. J., C. M. Kenyon, G. Ferrigno, P. Carnevali, A. Aliverti, A. Pedotti, P. T. Macklem, and D. F. Rochester.** Chest wall and lung volume estimation by optical reflectance motion analysis. *J. Appl. Physiol*. 81: 2680–2689, 1996.
6. **Campbell, E. J. M.** *The Respiratory Muscles and the Mechanics of Breathing*. Chicago, IL: Year Book, 1958.
7. **Campbell, E. J. M., and J. H. Green.** The behaviour of the abdominal muscles and intra-abdominal pressure during quiet breathing and increased pulmonary ventilation: a study in man. *J. Physiol. (Lond.)* 127: 423–426, 1955.
8. **Cerretelli, P., and P. E. Di Prampero.** Gas exchange in exercise. In: *Handbook of Physiology. The Respiratory System. Gas Exchange*. Bethesda, MD: Am. Physiol. Soc., 1987, sect. 3, vol. IV, chapt. 16, p. 297–339.
9. **Chihara, K., C. M. Kenyon, and P. T. Macklem.** Human rib cage distortability. *J. Appl. Physiol*. 81: 437–447, 1996.
10. **Closkey, R. F., A. B. Schultz, and C. W. Luchies.** A model for studies of the deformable rib cage. *J. Biomech*. 25: 529–539, 1992.
11. **Crawford, A. B., D. Dodd, and L. A. Engel.** Changes in rib cage shape during quiet breathing, hyperventilation and single inspirations. *Respir. Physiol*. 54: 197–209, 1983.
12. **De Troyer, A., M. Sampson, S. Sigrist, and P. T. Macklem.** The diaphragm: two muscles. *Science* 213: 237–238, 1981.
13. **Ferrigno, G., P. Carnevali, A. Aliverti, F. Molteni, G. Beulcke, and A. Pedotti.** Three-dimensional optical analysis of chest wall motion. *J. Appl. Physiol*. 77: 1224–1231, 1994.
14. **Goldman, M. D., G. Grimby, and J. Mead.** Mechanical work of breathing derived from rib cage and abdominal V-P partitioning. *J. Appl. Physiol*. 41: 752–763, 1976.
15. **Grimby, G., J. Bunn, and J. Mead.** Relative contribution of rib cage and abdomen to ventilation during exercise. *J. Appl. Physiol*. 24: 159–166, 1968.
16. **Grimby, G., M. D. Goldman, and J. Mead.** Respiratory muscle action inferred from rib cage and abdominal V-P partitioning. *J. Appl. Physiol*. 41: 739–751, 1976.
17. **Loring, S. H.** Action of human respiratory muscles inferred from finite element analysis of rib cage. *J. Appl. Physiol*. 72: 1461–1465, 1992.
18. **Loring, S. H., and J. Mead.** Action of the diaphragm on the rib cage inferred from a force-balance analysis. *J. Appl. Physiol*. 53: 756–760, 1982.
19. **Macklem, P. T., D. M. Macklem, and A. De Troyer.** A model of inspiratory muscle mechanics. *J. Appl. Physiol*. 55: 547–557, 1983.
20. **Macklem, P. T., L. Zocchi, and E. Agostoni.** Pleural pressure between diaphragm and rib cage during inspiratory muscle activity. *J. Appl. Physiol*. 65: 1289–1295, 1988.
21. **McCool, F. D., S. H. Loring, and J. Mead.** Rib cage distortion during voluntary and involuntary breathing acts. *J. Appl. Physiol*. 58: 1703–1712, 1985.
22. **McKenzie, D. K., S. C. Gandevia, R. B. Gorman, and F. C. Southon.** Dynamic changes in the zone of apposition and diaphragm length during maximal respiratory efforts. *Thorax* 49: 634–638, 1994.
23. **Mier, A., C. Brophy, M. Estenne, J. Moxham, M. Green, and A. De Troyer.** Action of abdominal muscles on rib cage in humans. *J. Appl. Physiol*. 58: 1438–1443, 1985.
24. **Mortola, J. P., M. Saetta, G. Fox, B. Smith, and S. Weeks.** Mechanical aspects of chest wall distortion. *J. Appl. Physiol*. 59: 295–304, 1985.
25. **Petroll, W. M., H. Knight, and D. F. Rochester.** Effect of lower rib cage expansion and diaphragm shortening on the zone of apposition. *J. Appl. Physiol*. 68: 484–488, 1990.
26. **Rahn, H., A. B. Otis, L. E. Chadwick, and W. O. Fenn.** The pressure volume diagram of the thorax and lung. *Am. J. Physiol*. 146: 161–178, 1946.
27. **Ringel, E. R., S. H. Loring, J. Mead, and R. H. Ingram, Jr.** Chest wall distortion during resistive inspiratory loading. *J. Appl. Physiol*. 58: 1646–1653, 1985.
28. **Saunders, N. A., S. M. Kreitzer, and R. H. Ingram, Jr.** Rib cage deformation during static inspiratory efforts. *J. Appl. Physiol*. 46: 1071–1075, 1979.
29. **Sharp, J. T., N. B. Goldberg, W. S. Druz, and J. Danon.** Relative contributions of rib cage and abdomen to breathing in normal subjects. *J. Appl. Physiol*. 39: 608–618, 1975.
30. **Verschakelen, J. A., K. Deschepper, and M. Demedts.** Relationship between axial motion and volume displacement of the diaphragm during VC maneuvers. *J. Appl. Physiol*. 72: 1536–1540, 1992.
31. **Ward, M. E., J. W. Ward, and P. T. Macklem.** Analysis of human chest wall motion using a two-compartment rib cage model. *J. Appl. Physiol*. 72: 1338–1347, 1992.